Article publicat / *Published paper*:

Lamich, M., Balcells, J., Corbalan, M., Griful, E. Nonlinear loads model for harmonics flow prediction, using multivariate regression. "IEEE transactions on industrial electronics", Juny 2017, vol. 64, núm. 6, p. 4820-4827. DOI10.1109/TIE.2017.2674596

Non linear Loads Model for Harmonics Flow Prediction, Using Multivariate Regression

Manuel Lamich, *Member, IEEE*, Josep Balcells, *Senior Member, IEEE* , Montserrat Corbalán*, Member, IEEE, and* Eulalia Griful

***Abstract*— This paper describes a method for obtaining a model of a single or a set of nonlinear loads (NLL) connected to a certain point of an electrical network. The basic assumption is that the network supplying the NLL has significant series impedances and is disturbed by other parallel, random and unknown neighbor loads, sharing part of the supply system with the NLL. The main interest for obtaining the model is its further use to predict the amount and flow of harmonic currents generated by the NLL, in the case of adding a filter to reduce the harmonics distortion. The modeling technique used in the paper is based on Multivariate Multiple Outputs Regression (MMOR) and leads to a set of equations giving the NLL behavior (one for each of the harmonic currents). The model is obtained from data taken at measuring point (MP) and is only valid to predict the NLL behavior when new loads are connected at this point. The modeling method was first tested with V, I data coming from simulations using Matlab-Simulink SimPowerSystems toolbox. Finally, the method has been validated using V, I data taken in a real installation with different neighbor loads and under different load conditions.**

***Index Terms*— Nonlinear Loads; Modeling; Harmonics; Power Quality; Multivariate Regression.**

I. Introduction

THE nonlinear loads (NLL) connected to industrial networks, mainly consisting of single-phase and three-phase rectifiers, cause distortion in the distribution networks, which increases as the short-circuit impedance increases [1][2]. That has led to the necessity of limiting the harmonic currents which can be generated by each utility user, according to certain international standards [3]-[5]. In case that a certain network section does not comply with such international rules, the user must include some filters to fix the problem of power quality in the network.

Usually, the simplest models of harmonics produced by rectifiers used in the literature, consider that such loads behave as ideal current sources (Norton model with infinite impedance) [6]-[12]. If such behavior were true, the harmonic currents generated by the nonlinear loads (NLL) would not depend on external circumstances such as: harmonics of the supply voltage, supply impedance, harmonics produced by other parallel disturbing loads or the eventual connection of an active or passive filter (APF) (Fig.1). Nevertheless in practice the harmonics amount and flow depend on all the above mentioned circumstances.

The real experiences show that the Norton model with infinite impedance can only be applied in case that the supply network has an infinite short-circuit capacity, which would mean that the harmonic currents generated by the NLL and by the neighbor loads, would not influence the supply voltage of the load being modeled. However, the presence of transformers and line impedances, shared by the NLL and other unknown loads (Z_S and neighbor loads in Fig.1), brings to a behavior where harmonic currents generated by the load of interest depend on such Z_S and neighbor loads.

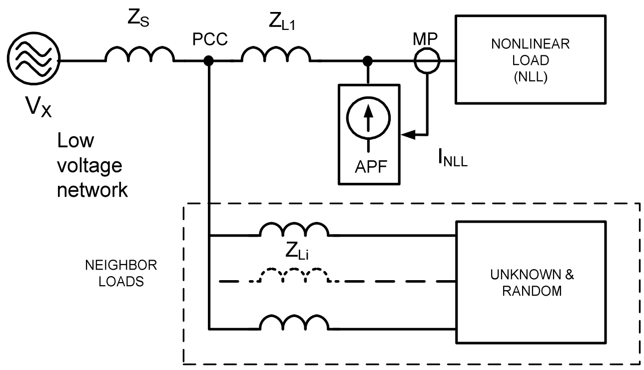

Fig. 1. Simplified network schematic including a hypothetic active filter (APF) at the measuring point (MP).

In order to take into account this non ideal behavior, some authors propose more accurate models based on Norton equivalent circuits with finite impedance for the NLL, combined with a Thevenin equivalent circuit, with a known internal impedance [13], to model the low voltage network. Others use analytical models based on the admittance matrix at the point of filter connection or measuring point (MP) [14]. Nevertheless, since the neighbor loads are usually unknown and random, it is very difficult to find a Thevenin-Norton or an admittance model which is valid for all the possible neighbor and load conditions. Moreover, as have described in

Manuscript received July, 28, 2016; revised December 12, 2016; accepted January 22, 2017. This work was supported in part by Ministerio de Economia y Competitividad, project TEC2011-25076 and project CD2009-00046 .

Manuel Lamich, Josep Balcells and Montserrat Corbalan are with the Departament d'Enginyeria Electrònica, Eulàlia Griful is with Department of Estadística i Investigació Operativa, both at Universitat Politècnica de Catalunya (UPC), Campus de Tarrassa (Barcelona), Spain (e-mail: manuel.lamich@upc.edu, josep.balcells@upc.edu, montserrat.corbalan@upc.edu , eulalia.griful@upc.edu).

[15], the insertion of a parallel filter at MP changes the supply conditions and modifies the NLL harmonics pattern and values, so usually, the model cannot be described by an admittance matrix obtained from a single set of voltage and current data.

Recently, several authors have proposed new methods, based on the admittance matrix, where the matrix coefficients are obtained from several sets of data representing the different NLL conditions and different environmental circumstances [16]-[21]. Beside the harmonic voltages and currents, which are the origin of the admittance matrix, such data sets may include other variables, as the NLL power, the total available power, etc., to better describe the load and the network. Many of the above mentioned papers [16]-[19], used Neural Networks (NN) for obtaining the relationship between harmonic currents and harmonic voltages (in fact the terms of admittance matrix) Nevertheless, the models based on NN have a drawback, e.g., there are many degrees of freedom: one can choose the number of neurons, the number and structure of layers, the type of neurons, etc., and there are not simple evaluation parameters to compare the models obtained from different NN. So, it is always difficult to know when the optimal model has been reached. Because of this, this paper explores the option of using more evaluable statistical procedures, namely, the Multivariate Multiple Outputs Regression (MMOR) to obtain the model of the NLL. The modeling procedure is explained in detail in [22] and gives a result consisting of a set of equations that can be put in matrix form, resulting in a sort of admittance matrix with some extra parameters, as explained below.

The input variables chosen to describe the model are: the fundamental and the harmonic voltages at the MP (Fig.1) and the active power drawn by the NLL. The output variables (model output) are the fundamental current and the harmonic currents generated by the NLL. Notice that both, voltages and currents, are phasors with two components: module and phase (in polar representation) or real and imaginary part (in Cartesian representation). Since the polar representation gives some problems when the phase of certain harmonics is close to $\pi/2$ [19], the Cartesian representation has been used.

The model will consist of a set of equations giving harmonic currents (I_h) as a function of harmonic voltages and power drawn by the NLL (V_h and P). Several sets of data are used to get the model coefficients (model training in the language of NN) , which will be described in detail in section III. The different data sets consist of arrays of (I_h, V_h, P), with h=1, 3, 5, 7, 9 …up to 15. Each array is for a different P and a different neighbor load (P_N).

Concerning the validation, it has been done in two stages: Method validation and field experimental validation.

The first stage was to validate the method and consisted of a model validation using data coming from a real circuit simulation. The second stage has been a true experimental validation, performed with real data collected at a ski resort installation. The first stage was considered necessary in order to validate the modeling method without the possible interferences of limited data resolution and measuring noise. In this first stage, the data used to get the model coefficients have had a nearly unlimited resolution. In the second stage the same data but with truncated resolution to 0,5V and 0,1A has been used. Finally we have made an experimental validation with data coming from real measurements, using a standard measuring instrument having a voltage resolution of about 1V (over 500V_{RMS} full scale) and whose current resolution was 0,1% in amplitude at full scale. Nevertheless, the current has been measured with a clamp, which can give significant phase errors for low current values. Because of that, we have only considered data above 5% of the rated power.

In section II we present the mathematical basis of the used methodology. Section III explains the generic schematic and the method for obtaining the training data in the simulation stage. Section IV explains, from a statistical point of view, the variables and data sets used for model training. Section V is devoted to obtain de NLL model matrix, section VI is dedicated to the model validation and finally in section VII there is a summary of the conclusions.

II. Multivariate Multiple Outputs Regression Method

The NLL model must be able to predict multiple outputs, namely the real and imaginary components of fundamental and harmonic currents, which will be generically designated as $Y_1, Y_2 \ldots Y_K$. Such outputs are functions of a set of inputs named: $X_1, X_2, \ldots X_J$,. Specifically, the input variables used in the MMOR model are the real and imaginary components of fundamental and harmonic voltages at the MP plus the NLL active power. In a first approach, we assume a linear model for each output (1),

$$Y_k = \beta_{0k} + \sum_{j=1}^{J} X_j \beta_{jk} + \varepsilon_k \quad k = 1,..,K \tag{1}$$

Where K is the number of outputs and J is the number of inputs.

The model will be obtained from N training cases, each consisting of a set of data (X_1, …, X_J, Y_1, …, Y_K) and therefore it can be described in the matrix notation as (2)

$$\mathbf{Y} = \mathbf{XB} + \mathbf{E} \tag{2}$$

Where **Y** is the $N\times K$ response matrix, where the nk entry is Y_{nk} . In our case the value of K is twice the number of harmonics which have to be predicted, since each harmonic is described by its real and imaginary parts and **X** is the $N\times(J+1)$ input matrix, including the harmonic voltages at the MP plus the NLL power, P. In our case $J=K+1$. B is the $(J+1)\times K$ matrix of coefficients (β_{jk}) and E is the $N\times K$ matrix of errors (ε_{nk}). Then, according to [22], the least squares estimates will be given by (3):

$$\hat{\mathbf{B}} = (\mathbf{X}^{\mathbf{T}}\mathbf{X})^{-1}\mathbf{X}^{\mathbf{T}}\mathbf{Y} \tag{3}$$

Hence the coefficients for the k_{th} outcome are just the least squares estimates in the regression of Y_k on $X_1, \ldots, X_J$.

Notice that from physical point of view, **B** is a matrix containing the coefficients relating harmonic currents to harmonic voltages, plus a row of coefficients relating harmonic currents with NLL power and a row of constant coefficients, β_{0k}, given in (1). Then **B** could be considered a sort of admittance matrix, with the above described extra rows.

According to [22], if the errors ($\varepsilon_1, \ldots \varepsilon_k$) in (1) are not correlated, the multiple outputs model can be solved as multiple single output least squares estimates. In this paper, the technique used to solve the model will be the Backward-Stepwise regression [22], consisting on selecting the best subset of (β_{jk}) which explains the model and guarantees a certain desired error level.

III. TRAINING DATA SET

As explained above, the NLL model is obtained from several sets of data recorded using different load and environmental conditions, which we call "training data". In a first approach, in this paper, we use a set of simulations of a generic circuit structure represented in Fig. 2 to get the training data. The simulations have been performed using Matlab-Simulink® and the SimPowerSystems® toolboxes.

The circuit in Fig. 2, represents a generic case, consisting of a Thevenin equivalent of the supply network formed by a voltage source (V_X) and a line impedance (Z_S) upstream of the point of common coupling (PCC).

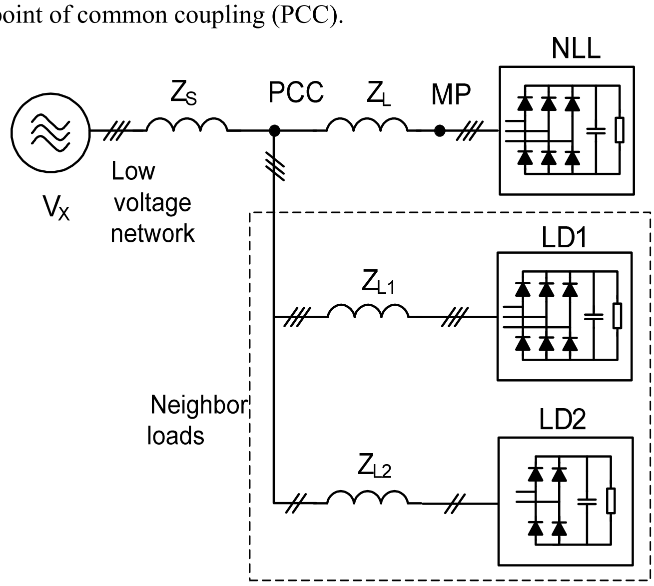

Fig. 2. Simulation block diagram.

From PCC there are several loads connected, namely, the nonlinear load (NLL) of interest and the unknown neighbor loads. It's assumed that neighbor loads can be represented by two blocks: LD1, gathering all the three phase loads (not using the neutral wire) and LD2 gathering all the single phase loads using the neutral wire. The NLL and the neighbor loads are connected to the same PCC as shown in Fig 2, where Z_L represents the line impedance between PCC and measuring point MP and Z_{L1} and Z_{L2} represent the line impedances from PCC to the different blocks of neighbor loads.

In the paper we consider that the NLL is a three phase rectifier or a set of three phase rectifiers and the set of neighbor loads (NL) consists of a mix of single and three phase rectifiers causing random variations of the voltage at the PCC and by extension at MP.

Training data sets were obtained using a random algorithm which assigns different values to the NLL power and to neighbor loads power. Specifically, 200 cases were simulated, with different combinations of nonlinear and neighbor load parameters. For each case we have an input vector (X_j) and an output vector (Y_k). The input vector consists of the harmonic voltages at MP plus the NLL power and the output vector consists of the harmonic currents at MP. In the training data generation process, the range of values for NLL current was set between five and sixty-five amperes and for LD1+LD2 (Fig.2) between twelve and sixty amperes. The particular combination of NLL and neighbor load for each case was chosen randomly within the above mentioned limits.

Despite data coming from simulation could have a nearly infinite resolution, we have truncated the resolution to 0.5V for voltages and to 0.1A for currents. We have done so, in order to test the modeling procedure in circumstances close to those found in real cases, where data come from network analyzers measuring voltages up to $500V_{RMS}$ and currents through a current clamp with a maximum resolution of 0.1% at full scale.

In principle, only the voltages and currents of odd harmonics up to the fifteenth were taken into account, since, after the truncation, the even harmonics and those above the fifteenth, were the same order of magnitude as noise and therefore they are negligible for our purposes. With the above described data conditions, the dimension of input vectors (X_j) was 17 (real and imaginary parts of odd harmonics V_1 to V_{15} plus the NLL power) and the dimension of output vectors (Y_k) was 16 (real and imaginary parts of odd harmonics I_1 to I_{15}).

IV. MODEL ESTIMATION AND STATISTICAL VALIDATION

As stated above, our simulated data set consisted of 200 cases. Such data set were split up into two parts: training and validation subsets (150 and 50 cases, respectively). With the training data set, we estimate the coefficients of sixteen models, corresponding to real and imaginary parts of harmonic currents (Y_k) as a function of seventeen potential input variables corresponding to real and imaginary parts of harmonic voltages and NLL power (X_j). The β_{0k}, β_{jk} coefficients of these models (see (1)) were estimated using the backward stepwise regression method.

The statistical validation was performed by evaluating three typical parameters used in null hypothesis testing [22]: the p-values, the R-squared values and the Mean Square Errors (MSE). In our example, the p-values of estimations were all less than 0.05 and the R-squared were all more than 0.99. This means that the models explain at least 99% of the variability of the output variables. All models have also been statistically validated from the point of view of residuals analysis and all MSE were less than 0.002.

As an example, in (4) we give the model equations for estimation of real and imaginary parts of the 5th harmonic current, corresponding to a certain NLL in a determined supply system,

$$\widehat{Re}(I_5) = -57{,}366 + 0{,}251\ Re(V_1) - 0{,}193\ Re(V_5) + 0{,}575\ Re(V_{11}) - 0{,}530\ Re(V_{15}) + 0{,}859\ Im(V_3) - 0{,}453\ Im(V_9) - 0{,}492\ Im(V_{13}) + 1{,}152\ \text{Power}$$

$$\widehat{Im}(I_5) = 89{,}247 - 0{,}394\ Re(V_1) - 0{,}697\ Re(V_3) - 2{,}531\ Im(V_3) + 1{,}298\ Im(V_7) - 0{,}117\ Im\ (V_{15}) + 1{,}605\ \text{Power} \qquad (4)$$

Notice that the model equations respond to the generic form given in (1), but we can observe the following:

a) Real and imaginary parts of a certain harmonic do not necessarily depend on the same input variables (namely the same real or imaginary parts of V_h).

b) Not all the input variables are significant for a certain harmonic. For example, in (4) only 9 out of 17 coefficients are significant for the real part and 7 out of 17 for the imaginary part.

V. Model Validation by Circuit simulation

The validation has been done by comparing the estimated harmonic currents given by the MMOR method with currents obtained from the circuit simulation (Fig.2). In all section V, we shall call "simulated" the values obtained from circuit simulation (by means of Matlab-Simulink SimPowerSystems) and "estimated" the values obtained from MMOR statistical model. The method used for validation was to compare the values of "simulated" and "estimated" outputs (fundamental and odd harmonic currents up to 15th). The set of "simulated" values were obtained from 50 circuit simulations within the training range (but not used for the training) plus 20 simulations having currents above the training range.

Despite the model was worked out in the frequency domain, the validation was performed both: in frequency domain and in time domain.

The basic criteria to validate the model was to compare different parameters, namely:

a) Comparison between simulated and estimated Total Harmonics Distortion *THD(I)%.*

b) Comparison between simulated and estimated values of real and imaginary components of each particular harmonic I_h.

c) Comparison between simulated and estimated temporal wave shapes of line current, obtained by using the inverse transformation of Fourier analysis.

These comparisons were performed separately for two different situations: a) Cases having currents within the training range, b) Cases having currents up to a 20% above the training range.

Of course, from a rigorous statistics point of view, we cannot pretend the model to be valid out of the range of training. Nevertheless, if the NLL has no current discontinuities (as might occur in arc furnaces, for instance) a certain linear behavior in the neighborhood of the training range can be assumed. This was checked during the validation process and the results were pretty good.

Fig. 3 shows the *THD(I)%* difference (5) between simulated and estimated values, using data with infinite resolution.

$$THD(I)_{error} = THD(I)_{sim} - THD(I)_{est} \qquad (5)$$

Where $THD(I)_{sim}$ and $THD(I)_{est}$ are the *THD* of the simulated and estimated currents respectively, both referred to its respective fundamental current.

Each spot of the Fig. 3 corresponds to a case. Blue spots correspond to cases used for model training, orange spots are cases within the training range, but not used for model training and black squares are estimated cases out of the training range. Fig. 4 shows the same *THD(I)%* difference, using data with resolution limited to 0.5V and 0.1A.

We can observe that the *THD(I)%* differences between simulated and estimated values are less than 1% for currents above 50% and high resolution, while for low resolution the differences increase to about 2%. Notice also that maximum errors occur for very low currents, which generally have a high *THD(I),* which indicates that errors are basically due to the lack of resolution in the current data.

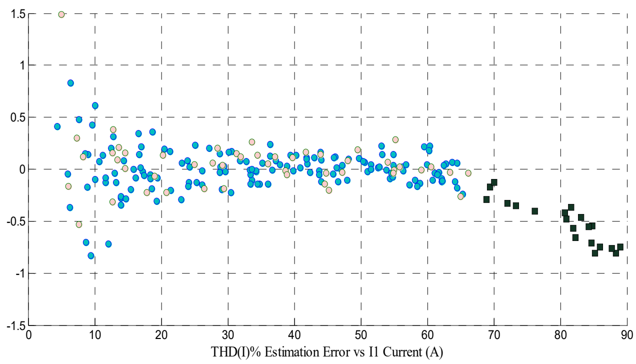

Fig. 3. Difference between estimated and simulated THD(I) with infinite resolution (dark squares correspond to cases out of the training range).

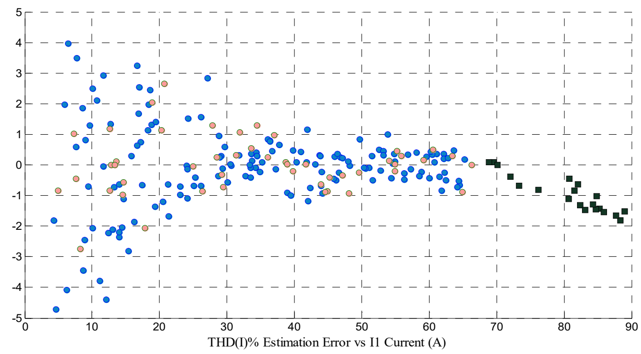

Fig. 4. Relative error between estimated and simulated THD(I) for truncated data resolution (dark squares correspond to cases out of the training range).

Fig. 5 shows the real and imaginary parts of harmonic currents for one of the worst cases within the training range. The differences between simulated and estimated currents are less than 0.2A over a peak current of 18A. Fig. 6 shows the temporal reconstruction for the same case as Fig. 5. Notice that both lines are overlapped. The differences in the worst point (close to zero) are less than 0.2A.

Fig. 7 shows the real and imaginary components of harmonic currents for a case where the NLL current is 20% above the training range. The differences between simulated and estimated currents are less than 0.4A over a peak current of 93A. Fig. 8 shows a temporal reconstruction of simulated and estimated currents for the same case as Fig. 7. Again the two lines are nearly overlapped. The differences in the worst case are less than 2A.

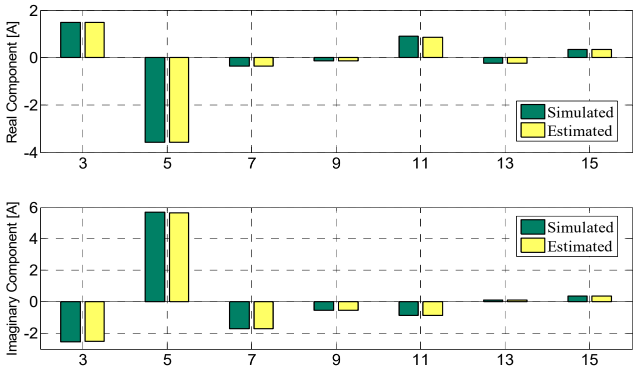

Fig. 5. Real and imaginary parts of simulated and estimated currents. Case_1, within the training range.

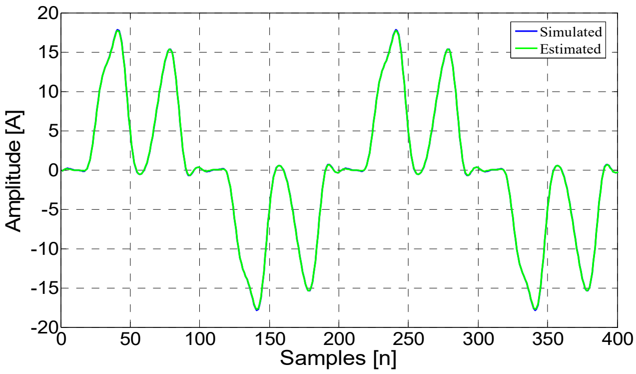

Fig. 6. Simulated and estimated currents reconstruction in time domain. Case_1, within the training range.

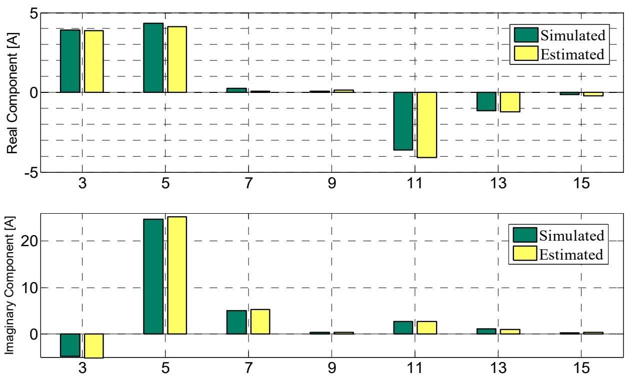

Fig. 7. Real and imaginary parts of simulated and estimated currents. Case_2, 20% out of the training range.

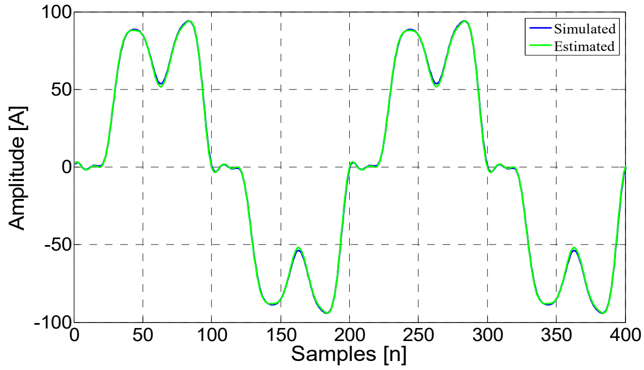

Fig. 8. Simulated and estimated currents reconstruction in time domain. Case_2, 20% out of the training range.

VI. Experimental Validation

In this section we give the details of an experimental validation performed with real data collected at a ski resort installation. Such installation is considered a typical case where there are weak lines (high impedance) and a powerful NLL mixed with some auxiliary neighbor loads. The installation has two groups of loads supplied by a 1000kVA transformer station. Specifically the groups are:

a) A big three phase Thyristor converter supplying a DC motor with a rated power of 160 kW. The drive is used to move a chairlift and, except for the early morning, normally works at 75 to 80kW. This is the NLL to model.

b) Several three phase and single phase lines, supplying auxiliary installations as hotel, bar, sport stores, lights, snow canons, etc. … considered to be the unknown neighbor loads.

Training data come from real measurements in such installation, using a standard supply network analyzer having a voltage resolution about 1V (over $500V_{RMS}$ full scale) and a current resolution of 0.1A. We followed a validation procedure similar to that used for data in section V. We took a set of 135 recordings, made a first estimation model and we saw that the reactive current and the harmonic currents seemed to be grouped in two subsets of cases. Fig. 9.a shows the reactive current and Fig. 9.b shows the 5^{th} harmonic real term versus active power.

Both graphs in Fig. 9 suggest that there are two different groups of behavior of the NLL. Further investigations revealed that the difference have been that there was a PF correction equipment based on the connection of capacitors in two steps. From this point two different models for the two subsets of cases were made. Fig. 10 shows the THD(I) error for the two subsets.

Fig. 11 and Fig 13 display the real and imaginary parts of harmonic currents for two cases not used in the models training.

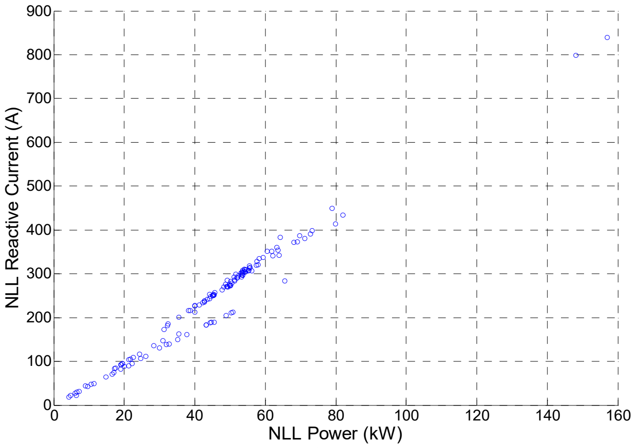

a)

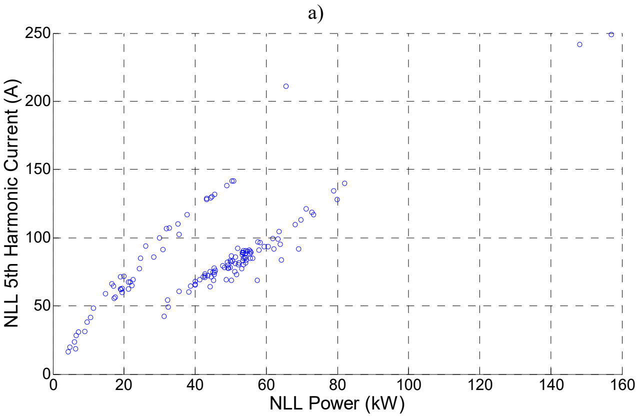

b)

Fig. 9. a) Reactive current and b) 5th harmonic current versus NLL power.

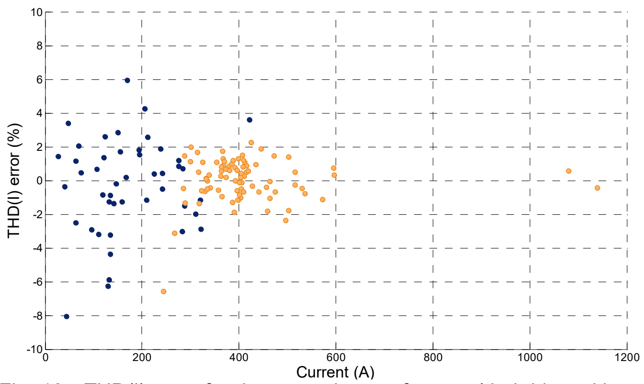

Fig. 10. THD(I) error for the two subsets of cases (dark blue without PF compensation, orange with PF compensation).

Fig. 12 and Fig. 14 show the comparison between estimated and measured current waveforms for two reconstruction cases, not used in the models training. A nearly perfect agreement in case of high currents and higher errors in case of low currents can be seen. This has been attributed to the lack of resolution of voltage and current measurements.

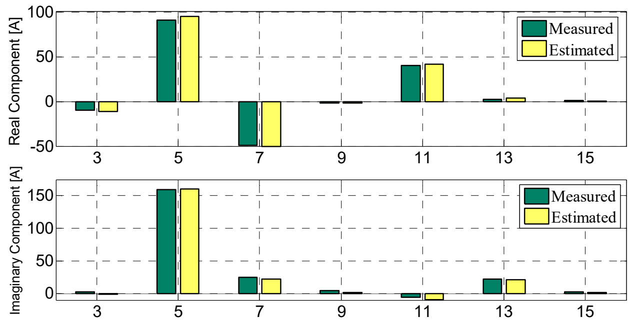

Fig. 11. Real and imaginary parts of measured and estimated currents. Case without PF compensation

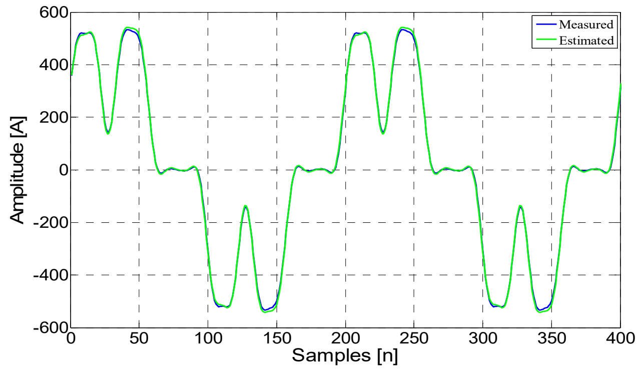

Fig. 12. Measured and estimated currents reconstruction in time domain. Case without PF compensation

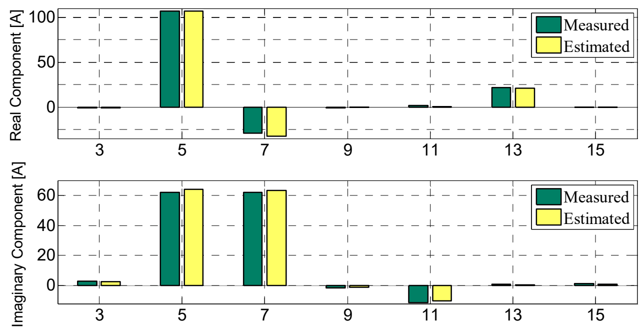

Fig. 13. Real and imaginary parts of measured and estimated currents. Case with PF compensation

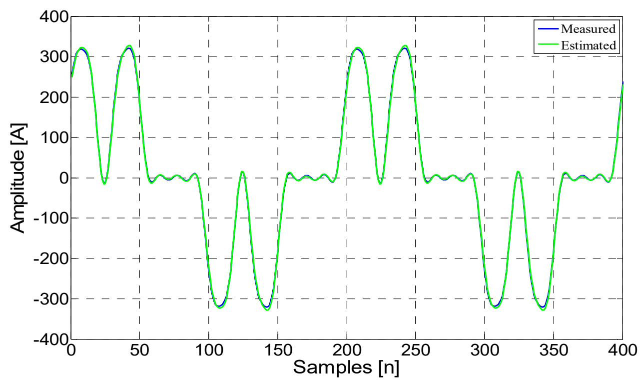

Fig. 14. Measured and estimated currents reconstruction in time domain. Case with PF compensation

VII. Conclusions

In this paper, we have tested the Multivariate Multiple Outputs Regression (MMOR) technique for obtaining a model for the estimation of harmonic currents generated by nonlinear loads (excluding those involving arc phenomena), taking into account the random behavior of unknown neighbor loads.

The novelty using this technique is that it allows obtaining explicit equations of the model and gives additional statistical parameters to evaluate the goodness of the model. This is an important advantage of MMOR compared to the method used in a previous work based on NN.

As other techniques, MMOR requires a set of data, containing the output results, in order to "train" the model. Notice that model equations are only valid for the NLL connected to a precise point, that we named MP.

The method also allows detecting different groups of NLL behavior, as demonstrated in the experimental validation. If such groups are treated concurrently, the MMOR procedure tries to give an average model whose predictions have higher deviations. But splitting up the groups of behavior and making separate models for them gives more accurate estimation models.

Model validation has been done with simulated and experimental data, in the time and frequency domains, showing, in both cases, a very good agreement between the model and the measured data.

The paper also shows that the method requires a certain minimum resolution of data used for training. Due to that, the predictions for very low currents, in the lower part of the measuring range, lead to relatively high errors, but predictions in the top part of the current range or even slightly above the training range give models with a very high accuracy.

References

[1] B. Singh, K. Al-Haddad, and A. Chandra; "A Review of Active Filters for Power Quality Improvement," *IEEE Trans. Ind. Electron*., vol. 46, no.5, pp. 960 – 971, Oct.1999.

[2] L. Sainz, J. J. Mesas, and A. Ferrer, "Characterization of non-linear load behavior," *Elect. Power Syst. Res*., vol. 78, no. 10, pp. 1773–1783, Oct. 2008.

[3] Electromagnetic compatibility (EMC) - Part 3-2: Limits - Limits for harmonic current emissions (equipment input current <= 16 A per phase), EN 61000-3-2, CENELEC 2006.

[4] Electromagnetic compatibility (EMC) - Part 3-12: Limits - Limits for harmonic currents produced by equipment connected to public low-voltage systems with input current >16 A and ? 75 A per phase, EN 61000-3-12, CENELEC 2011.

[5] IEEE Recommended Practice and Requirements for Harmonic Control in Electric Power Systems, IEEE STANDARD 519, 2014.

[6] E. Thunberg and L. Soder, " A Norton Approach to Distribution Network Modeling for Harmonic Studies," *IEEE Trans. Power Del*., vol. 14, no. 1, pp. 272 – 277, Jan. 1999.

[7] C-S. Lam, M-C Wong, W-H Choi, X-X Cui, H-M Mei, and J-Z Liu," Design and Performance of an Adaptive Low-DC-Voltage-Controlled LC-Hybrid Active Power Filter With a Neutral Inductor in Three-Phase Four-Wire Power Systems," *IEEE Trans. Ind. Electron.*, vol. 61, no. 6, pp. 2635 - 2647, June 2014.

[8] L. Herman, I. Papic and B. Blazic, "Proportional-Resonant Current Controller for Selective Harmonic Compensation in a Hybrid Active Power Filter"; *IEEE Trans. Power Del*., vol. 29, no. 5, pp. 2055 - 2065, Oct. 2014

[9] A. F. Zobaa, "Optimal Multiobjective Design of Hybrid Active Power Filters Considering a Distorted Environment," IEEE Trans. Ind. Electron, vol. 61, no. 1, pp. 107 – 114, Jan. 2014.

[10] LR. Limongi, LR. da Silva, LGB. Genu, F. Bradaschia and MC. Cavalcanti, "Transformerless Hybrid Power Filter Based on a Six-Switch Two-Leg Inverter for Improved Harmonic Compensation Performance", *IEEE Trans. Ind. Electron.*, vol. 62, no. 1, pp.40-51, 2015.

[11] RL. De Araujo Ribeiro; TOA. de Rocha; RM. de Sosa; EC. dos Santos and AM. Nogueira, " A Robust DC-Link Voltage Control Strategy to Enhance the Performance of Shunt Active Power Filters Without Harmonic Detection Schemes", IEEE Trans. Ind. Electron., vol. 62, no. 2, pp.803-813, 2015.

[12] A. Javadi, A. Hamadi, L. Woodward and K. Al-Haddad, "Experimental Investigation on a Hybrid Series Active Power Compensator to Improve Power Quality of Typical Households", *IEEE Trans. Ind. Electron.*, vol. 63, no. 8, pp.4849-4859, 2016.

[13] H. Wu, W. Deyu, G. Xiaoqiang, S. Guocheng, Z. Wei, Z. Ying, W. Weiyang, "Two-degree-of-freedom current regulation of grid-connected inverters in microgrid," 2nd IEEE Int. Symp. on Power Electron. for Distributed Generation Syst. (PEDG), Hefei, China, 16-18 Jun., 2010, pp. 512 - 515.

[14] M. Fauri, "Harmonic Modelling of Nonlinear Load by Means of Crossed Frequency Admittance Matrix," *IEEE Trans. Power Syst*., vol. 12, no. 4, pp. 1632 - 1638, Nov. 1997.

[15] L. Sainz, J. Balcells, "Harmonic Interaction Influence Due to Current Source Shunt Filters in Networks Supplying Nonlinear Loads"; *IEEE Trans. Power Del.*, vol. 27, no. 3, pp. 1385 - 1393, July 2012.

[16] J. Mazumdar and R. G. Harley, "Recurrent Neural Networks Trained With Backpropagation Through Time Algorithm to Estimate Nonlinear Load Harmonic Currents", *IEEE Trans. Ind. Electron.*, vol. 55, no. 9, pp.3484-3491, Sept. 2008.

[17] J. Dai, P. Zhang, J. Mazumdar, R.G. Harley, and G.K. Venayagamoorthy, "A comparison of MLP, RNN and ESN in determining harmonic contributions from nonlinear loads," *34th Annu. Conf. of IEEE, Ind. Electron., IECON 2008*, Orlando, FL, 10-13 Nov., 2008, pp. 3025 - 3032.

[18] M. Lamich, J. Balcells, M. Corbalán, L. Sainz, C. Fernandez, "Modeling harmonics of networks supplying nonlinear loads," *IEEE 23rd Int. Symp. Ind. Electron.*, ISIE 2014, Istanbul, 1-4 Jun., 2014, pp.2030-2034.

[19] M. Lamich, J. Balcells, J. Mon, M.Corbalán, and E. Griful, "Modelling harmonics drawn by nonlinear loads," *9th Int. Conf. on Compatibility and Power Electron. (CPE)*, Costa da Caparica, Lisbon; 24-26 Jun., 2015, pp. 93 - 97.

[20] Farzad Karimzadeh, Saeid Esmaeili, and Seyed Hossein Hosseinian; "A Novel Method for Noninvasive Estimation of Utility Harmonic Impedance Based on Complex Independent Component Analysis"; IEEE Transactions on Power Delivery, Vol. 30, No. 4, August 2015; pp 1843-1852.

[21] Qi Fei, Li Jian-wen, Li Yong-gang, Sun Wei, Li Zhong-liang ; "Research on the Responsibility Partition of Harmonic Pollution and Harmonic Impedance Based on the Total Least-squares Regression Method"; 2014 International Conference on Power System Technology (POWERCON 2014) Chengdu, 20-22 Oct. 2014.

[22] T. Hastie, R Tibshirani and J Friedman, *The Elements of Statistical Learning: Data Mining, Inference, and Prediction*, 2nd ed, Springer Series in Statistics, 2009.

Manuel Lamich (M'97) was born in Tarragona, (Spain), received his BS degree from Universitat Laboral de Tarragona in 1990 and the Master Engineering degree in 1995 and the Ph.D in 2015 from Universitat Politècnica de Catalunya (UPC). From 1995 to 2003 he was assistant professor and since 2003 to 2016 he was associated professor and he is currently professor at Electronics Engineering Dept. in UPC. He has participate in several research projects founded by Spanish Ministry of Ciencia y Tecnología and has participated in others funded by the European Union in the V, VI and VII Frame Programs. His topics of interest are: Power Electronics, EMC in power systems, power quality and digital signal processing.

Josep Balcells, (M'94-SM'06) was born in Vila-rodona ,Tarragona (Spain), received the Master Engineering degree in 1975 and the Ph.D in 1983 from Universitat Politècnica de Catalunya (UPC). From 1975 to 1986 he was associated professor and since 1986 he is professor at Electronics Engineering Dept. in UPC. From 1976 to 1986 he was the head of R&D in Power Electronics in AGUT SA (now a GE group company) and from 1986 to 2015 he was technical consultant of CIRCUTOR SA. He has leaded several research projects founded by Spanish Ministry of Ciencia y Tecnología and has participated in others funded by the European Union in the V, VI and VII Frame Programs. His topics of interest are: Power Electronics, EMC in power systems, measurement and filtering of disturbances produced by power converters. From 2004 to 2015, he served as Associate Editor of the IEEE Transactions on Industrial Electronics.

Montse Corbalán (M'10), was born in Teruel (Spain), received the B.S. and M.S. degrees in physics from the Universitat Autónoma de Barcelona, Spain, in 1990 and 1993, respectively, and the Ph.D. degree in physics from the Universitat Politècnica de Catalunya (UPC), Spain, in 1997.
Since 1991, she has been with UPC, first as an Assistant Professor with the Department of Physics and Nuclear Engineering and then, since 2002, as an Associate Professor with the Department of Electronic Engineering. She has worked on optical pattern recognition of color images, digital signal processing, and methods for characterizing cameras and color. She has also worked on quality assessment and assurance in higher education. Currently, her research interests include digital signal processing, power electronics, power quality and quality assessment and assurance in higher education.

Eulàlia Griful was born in Barcelona, Spain. She graduated in Mathematics and received the Ph.D. degree from Universitat de Barcelona (UB) in 1981 and 1990 respectively. She has been an Associate Professor at the Department of Statistics and Operations Research of Universitat Politècnica de Catalunya Barcelona TEC (UPC) since 1991. She has served as deputy director of Academic Innovation (2001-2007) and director of the School of Industrial and Aeronautics Engineering of Terrassa (2007-2013). Her main research interests include applied statistical techniques for the quality management, reliability assessment and metrological control of industrial devices and equipment.